Selectivity of externally facing ion-binding sites in the Na/K pump to alkali metals and organic cations

Ian M. Ratheal[a,1], Gail K. Virgin[a,b,1], Haibo Yu[c], Benoît Roux[c], Craig Gatto[b], and Pablo Artigas[a,2]

[a]Department of Cell Physiology and Molecular Biophysics, Texas Tech University Health Sciences Center, Lubbock, TX 79430; [b]School of Biological Sciences, Illinois State University, Normal, IL 61790; and [c]Department of Biochemistry and Molecular Biology, University of Chicago, Chicago IL 60637

Edited by Chikashi Toyoshima, University of Tokyo, Tokyo, Japan, and approved September 14, 2010 (received for review April 1, 2010)

The Na/K pump is a P-type ATPase that exchanges three intracellular Na^+ ions for two extracellular K^+ ions through the plasmalemma of nearly all animal cells. The mechanisms involved in cation selection by the pump's ion-binding sites (site I and site II bind either Na^+ or K^+; site III binds only Na^+) are poorly understood. We studied cation selectivity by outward-facing sites (high K^+ affinity) of Na/K pumps expressed in *Xenopus* oocytes, under voltage clamp. Guanidinium$^+$, methylguanidinium$^+$, and aminoguanidinium$^+$ produced two phenomena possibly reflecting actions at site III: (*i*) voltage-dependent inhibition (VDI) of outwardly directed pump current at saturating K^+, and (*ii*) induction of pump-mediated, guanidinium-derivative–carried inward current at negative potentials without Na^+ and K^+. In contrast, formamidinium$^+$ and acetamidinium$^+$ induced K^+-like outward currents. Measurement of ouabain-sensitive ATPase activity and radiolabeled cation uptake confirmed that these cations are external K^+ congeners. Molecular dynamics simulations indicate that bound organic cations induce minor distortion of the binding sites. Among tested metals, only Li^+ induced Na^+-like VDI, whereas all metals tested except Na^+ induced K^+-like outward currents. Pump-mediated K^+-like organic cation transport challenges the concept of rigid structural models in which ion specificity at site I and site II arises from a precise and unique arrangement of coordinating ligands. Furthermore, actions by guanidinium$^+$ derivatives suggest that Na^+ binds to site III in a hydrated form and that the inward current observed without external Na^+ and K^+ represents cation transport when normal occlusion at sites I and II is impaired. These results provide insights on external ion selectivity at the three binding sites.

ion selectivity | Na,K-ATPase | pump current | voltage-dependent | guanidinium

The Na/K pump uses the free energy from ATP hydrolysis to export three Na^+ ions against a steep electrochemical gradient in exchange for the import of two K^+ ions. The pump alternates between two major conformational states, E1 and E2 (1), and its function is explained via a ping-pong (2) alternate-access mechanism (Fig. S1). Under physiological conditions, the E2P (phosphorylated) state, with extracellular-facing ion-binding sites, must select K^+ in the presence of more than 10-fold greater external Na^+ concentration. On the other hand, the E1 state, with cytoplasmic-facing ion-binding sites, selects Na^+ over K^+, which is present at a 10-fold higher concentration.

Of the three ion-binding sites, sites I and II, or shared sites, can bind either Na^+ or K^+, but site III exclusively binds Na^+. External release of Na^+ ions from these three sites occurs sequentially (3, 4). In the outward-facing conformation, Na^+ release is followed by binding of K^+ in the normal forward operation of the Na/K pump, inducing an outwardly directed pump current that can be studied under voltage clamp. Rebinding of Na^+_o to outward-facing sites in the presence of K^+_o induces voltage-dependent inhibition (VDI) at negative voltages, observed as a positive slope in the pump current–voltage (I_P–V) plots (5, 6). Because of the sequential nature of Na^+ release, this end-product inhibition by Na^+_o is complex, involving competition for the shared sites at nonsaturating $[K^+_o]$ as well as noncompetitive inhibition caused by binding to the Na-exclusive site.

Most of the cycle's voltage dependence is believed to arise from the release (rebinding in the backward reaction) of the first Na^+ ion through a high-field access channel when leaving its binding site (3, 4, 7). There are indications that the Na^+-exclusive site III releases Na^+ before the shared sites (6, 8, 9) and that the voltage-dependent rebinding of this first externally released Na^+ blocks release of the other two Na^+ ions from the shared sites. Concordantly, at saturating $[K^+_o]$, where Na^+ competition for the shared sites should be negligible, the Na/K pump current still presents significant VDI in the presence of external Na^+ (10) (Fig. S2). In addition, several studies have proposed a noncanonical mode of transport in which protons move in the inward direction down their electrochemical gradient at very negative voltages (11) through a pathway that passes through site III (9, 10, 12, 13).

These observations raise a number of critical questions about the underlying physicochemical factors governing ion selectivity of the shared and exclusive cation sites and about how these factors affect the directionality of the Na/K pump conformational transitions. The recent crystallographic structure of the Na/K pump at 2.4-Å resolution shows the coordination of two K^+ ions in the tightly bound E2 conformation (14). Nevertheless, it remains unclear how the pump dynamically selects among different cations and why the binding of K^+ or Na^+ at the extracellular sites induces a forward or reverse cycle, respectively.

We used an approach directly inspired by classical electrophysiological studies of ion selectivity in voltage-dependent channels (15) to deepen our understanding of the structural and energetic factors governing ion selectivity in the shared and exclusive sites by examining the functional effects of substituting a broad range of metal and organic cations for Na^+_o or K^+_o. Interest in the effect of organic cations was motivated by previous observations showing that guanidinium^+_o (Gua^+_o) produces voltage-dependent inhibition of outward (3Na/2K stoichiometric) pump current (I_P) at very negative voltages, indicating that this organic cation is able to enter the high-field access channel to reach site III with lower affinity than Na^+ (10). The present results suggest that some Gua^+ derivatives also can transit the access channel responsible for VDI, whereas acetamidinium$^+$ ($Acet^+$) and formamidinium$^+$ ($Form^+$) operate as K^+_o surrogates at the shared binding sites and are transported by the pump in exchange for Na^+_i. By deciphering the structural requirements for an ion to bind both at the Na^+-exclusive and the Na/K shared sites, these findings broaden previously viewed constraints, contributing to understanding the molecular determinants of external cation selectivity by the Na/K pump.

Author contributions: B.R., C.G., and P.A. designed research; I.R., G.V., and H.Y. performed research; I.R., G.V., H.Y., and P.A. analyzed data; and B.R., C.G., and P.A. wrote the paper.

The authors declare no conflict of interest.

This article is a PNAS Direct Submission.

[1]I.R. and G.V. contributed equally to this work.

[2]To whom correspondence should be addressed. E-mail: Pablo.Artigas@ttuhsc.edu.

This article contains supporting information online at www.pnas.org/lookup/suppl/doi:10.1073/pnas.1004214107/-/DCSupplemental.

Results

Ion Selectivity of the Na-Exclusive Site and Its Access Pathway. Steady-state currents mediated by the Na/K pump in Na-loaded *Xenopus* oocytes under two-electrode voltage clamp were identified as those inhibited by 10 mM ouabain (a specific inhibitor). First, we measured the ion selectivity of VDI of the outwardly directed (positive) I_P that occurs in the presence of near-saturating K^+_o (10 mM) because of the stoichiometric exchange of $3Na^+_i$ for $2K^+_o$ (Fig. 1). Fig. 1*A* shows the I_P–V curve with 120–125 mM of several organic cations, whose structures are shown in Fig. S2. A steep positive slope, nearly absent in *N*-methyl-D-glucamine^+_o (NMG^+_o), was clearly observed in Gua^+_o. Two other cations, $Form^+_o$ and methylguanidinium^+_o ($Mgua^+_o$) showed an intermediate inhibition at negative voltages. Fig. 1*B* illustrates similar experiments performed with 125 mM of various alkali metals. Cs^+_o and K^+_o present I_P–V curves that resemble control (125 mM NMG^+_o), whereas currents in Li^+_o and Na^+_o present significant inhibition at negative voltages. The higher the affinity of an ion for the VDI site, the more the I_P–V curve moves to the right. Thus, a convenient estimation of VDI, the ratio between pump current measured at −200 and at 0 mV ($I_{P,-200}/I_{P,0}$), was calculated for the different external cations (Fig. 1*C*). Na^+_o, Li^+_o, and Gua^+_o produced the most (~70–80%) inhibition, followed by $Mgua^+_o$, aminoguanidinium^+_o ($Agua^+_o$), and $Form^+_o$ with intermediate (~50%) inhibition and by NMG^+_o, methylamine^+_o (MA^+_o), Cs^+_o, and K^+_o with minimal (~25%) inhibition.

Na/K pump currents are relatively small (~200 nA at 0 mV) (10), and VDI in Na^+_o is only ~50% higher than that observed in NMG^+_o (our inert reference cation), making it difficult to obtain reliable quantitative conclusions regarding effects of other cations. In particular, because of the large inward current in the absence of K^+_o and the presence of 120 mM Gua^+_o (~10-fold larger than maximal outward I_P (10), we considered whether Gua^+_o reduced the apparent affinity for K^+_o, resulting in a fraction of K^+-free pumps with enough inward (negative) current to cause a positive slope on the curve and giving the false impression of VDI of outward I_P. Indeed, Gua^+_o (120 mM) increased the half-maximal constant for activation of outward current ($K_{0.5}$) for K^+_o approximately fourfold compared with NMG^+_o (Fig. S3). Nonetheless, when K^+_o was increased to 20 mM (where K^+ occupancy would be 0.995; $K_{0.5}$ = 0.6 mM; n_H = 1.5) (Fig. S3), VDI in Gua^+_o still was 35% higher than in NMG^+_o and 15% less than in Na^+_o (Fig. S4). The voltage dependence of the maximal K^+_o-activated outward current in Na^+_o solution (calculated from Hill fits) illustrates that 20 mM K^+_o is saturating even in the presence of Na^+_o.

VDI of I_P by Na^+_o at high K^+_o and inward current in the absence of Na^+_o and K^+_o may represent two different actions involving access to site III. Therefore, we tested whether the larger currents observed in Gua^+_o compared with NMG^+_o (10) represent Gua^+ permeation through the pump. To this end, we measured the pH_o dependence of ouabain-sensitive current with 120 mM NMG^+_o and 120 mM Gua^+_o solutions (Fig. 2*A*), as well as the $[Gua^+_o]$ dependence of currents at pH_o 8.6 (Fig. 2*B*). Fig. 2*A* displays the average pump-mediated I_{ouab}–V curves normalized for different expression levels. An ouabain-sensitive outward current observed in NMG^+_o solutions at pH_o 8.6 may represent efflux of uncoupled Na^+, whose stoichiometry and electrogenicity in other preparations is known to change with pH (16). The outward current was inhibited at all voltages by lowering pH_o to 7.6, and an inward current developed at negative voltages. The reversal potential (V_{rev}) of this current shifted toward more positive potentials as the $[H^+_o]$ was raised (V_{rev} ~ −30 mV at pH 7.6; V_{rev} ~ −7 mV at pH 6.6) (Fig. 2*A*, *Inset*), confirming that H^+ (or H_3O^+) is the main charge carrier for this current in NMG^+_o solution, as previously shown (11). The pH_o dependence of inward current in Gua^+_o was different, with V_{rev} close to 0 mV at all explored pH_o values (V_{rev} = 0 mV at pH_o 8.6; V_{rev} = −7 mV at pH_o 7.6; and V_{rev} = +10 mV

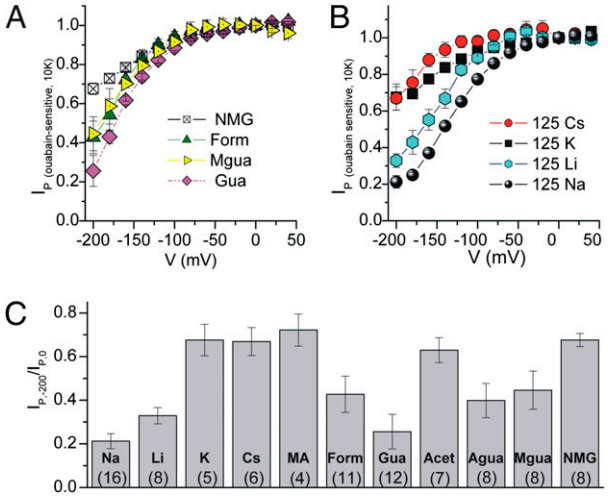

Fig. 1. Voltage dependence of normal Na/K pump currents (I_P). Square voltage pulses (50 ms) ranging from −200 to +40 mV [20-mV increments; holding potential (V_h) = −50 mV] were applied in voltage-clamped oocytes bathed in solutions containing the indicated external cations with 10 mM K^+_o. Experiments were performed in the absence or presence of 10 mM ouabain. The mean ouabain-sensitive I_p during the last 5 ms at each voltage from 6 to 15 oocytes from different frogs was normalized to the current induced by 10 mM K^+_o at 0 mV in NMG^+_o, averaged, and plotted against test voltage for solutions containing (*A*) 120 mM of the indicated organic cations or (*B*) 125 mM of the indicated alkali metals. (*C*) Average current remaining at −200 mV (I_{P-200}/I_{P0}) with cations Li, Na, Cs, MA, Form, Acet, Gua, Agua, Mgua, and NMG. Means ± SEM are from (*n*) experiments.

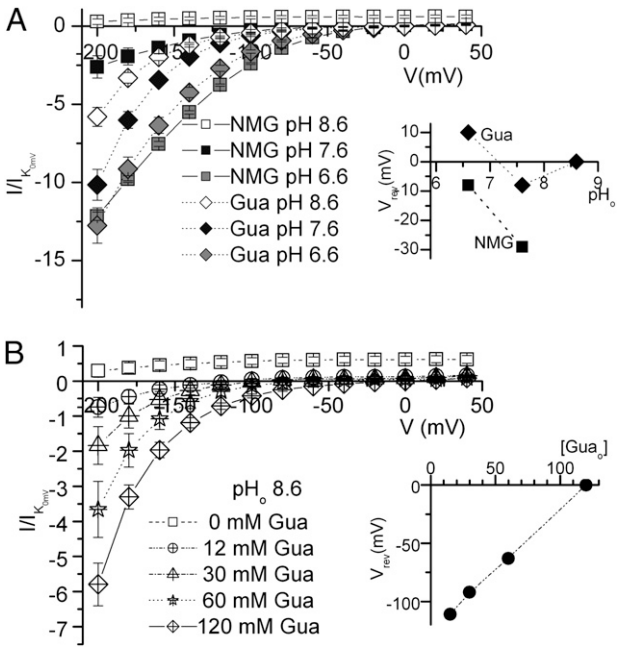

Fig. 2. $[H^+_o]$ and $[Gua^+_o]$ dependence of uncoupled currents through Na/K pumps. (*A*) I–V relationships of ouabain-sensitive currents in the absence of Na^+_o and K^+_o in solutions containing 120 mM NMG^+_o (squares) or 120 mM Gua^+_o (diamonds) at pH 7.6 (black), pH 6.6 (gray), or pH 8.6 (open symbols). (*Inset*) The visually estimated by the B-spline line connecting the average data (V_{rev}) as a function of pH_o in each external solution. (*B*) I–V curves (pH_o 8.6) with varying $[Gua^+_o]$. (*Inset*) V_{rev} (estimated as in *A*) as a function of $[Gua^+_o]$. Data points are means ± SEM of 5 to 15 experiments in each condition. Currents were normalized to the current induced by 10 mM K^+_o in NMG^+_o at 0 mV.

PHYSIOLOGY

at pH_o 6.6) (Fig. 2*B*, *Inset*), suggesting that in 120 mM Gua^+_o, H^+ ions are not the main charge carrier. The [Gua^+_o] dependence of ouabain-sensitive current at pH_o 8.6 (Fig. 2 and Fig. S5) shows that V_{rev} shifted from ~−110 mV at 12 mM Gua^+_o, increasing progressively with the [Gua^+_o], to ~0 mV at 120 mM Gua^+_o (Fig. 2*B*, *Inset*), indicating that Gua^+_o is indeed the main charge carrier at this pH_o.

To address the molecular constraints on this pump-mediated passive cation flux, we measured ouabain-sensitive currents in the presence of 120–125 mM of other cations at pH_o 7.6 without K^+_o (Fig. 3). Fig. 3*A* shows the voltage dependence of currents measured in oocytes bathed with several organic cations. The inward current in $Mgua^+_o$ or $Agua^+_o$ was significantly larger than in NMG^+_o, and an ouabain-sensitive [$Mgua^+_o$]-dependent inward current also was evident at pH_o 8.6 (Fig. S6), indicating permeability of this large cation. In contrast, $Acet^+_o$ and $Form^+_o$ produced outward currents rather than the expected inward current (Fig. 3*A*).

Ion Selectivity of the Shared Sites. The voltage dependence of the outward currents observed with 120 mM $Acet^+$ or 120 mM $Form^+$ is displayed on an expanded current scale in Fig. 3*B*, together with the curves observed with 125 mM of alkali metals. Cs^+ and Li^+ are well-known K^+ surrogates at external sites of the Na/K pump (1), and the curves in $Form^+_o$ and $Acet^+_o$ fall between those obtained with Cs^+ and Li^+, whereas the curve in Na^+_o shows no outward current. The current in 120 mM $Acet^+_o$ was larger than in $Form^+_o$, particularly at negative voltages, consistent with $Acet^+_o$ producing less VDI than $Form^+_o$ (Fig. 1*C*). $Form^+_o$ was more similar to Li^+_o (which also is known to act as a Na^+ surrogate on the pump) (17), in that it induced significantly less outward current than K^+_o, with a steeper positive slope.

To explore these K^+-like effects further, we measured the [ion^+_o] dependence of outward current activation (Fig. 4). Fig. 4*A* illustrates a continuous recording from an oocyte held at −50 mV. Step increments in [$Form^+_o$] increased the current in a saturable fashion. Addition of 10 mM K^+_o to the 120 mM $Form^+_o$ solution induced very small extra outward current (Fig. 4*A*). Fig. 4*B* shows the voltage dependence of the $K_{0.5}$ for outward current activation by different cations obtained from experiments analogous to Fig. 4*A*, in which ion-induced outward currents were measured at the end of 50-ms voltage pulses (seen as vertical deflections of the current in the compressed time scale of Fig. 4*A*). Atomic absorption confirmed that these outward currents induced by $Acet^+_o$ and $Form^+_o$ were not caused by contaminating K^+_o ([K^+_o] ≤ 0.003 μM at 120 mM organic cation; $K_{0.5,K}$ = 130 μM in NMG^+_o).

The unexpected results with $Form^+_o$ and $Acet^+_o$ suggest that the Na/K pump may recognize and import these ions as K^+_o congeners. Ouabain-sensitive ATPase measurements were performed on purified sheep kidney Na,K-ATPase to test this possibility directly in a classical preparation of native (α1/β1) Na/K ATPase. Both $Acet^+_o$ and $Form^+_o$ induced cation$^+$-dependent ouabain-sensitive ATPase activity with an extrapolated maximal velocity similar to K^+_o (Fig. 5*A*). (The reduced apparent affinity for cations compared with Fig. 4 is caused by the presence of 30 mM Na^+ in the ATPase medium.) To demonstrate unequivocally that the Na/K pump can transport these organic cations, we measured ^{14}C-$Acet^+$ uptake in oocytes overexpressing ouabain-sensitive wild-type α1+β3 pumps (Fig. 5*B*). Uptake was significantly (approximately twofold) larger in the absence of ouabain than in its presence ($P < 0.01$, independent *t* test). Thus, $Acet^+_o$ and $Form^+_o$ act as K^+_o surrogates on the Na/K pump.

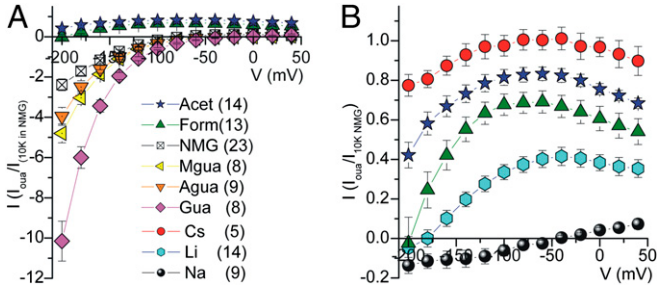

Fig. 3. Ion selectivity of Na/K pump-mediated currents in the absence of K^+_o. Ouabain-sensitive I–V relationships measured in voltage-clamped oocytes bathed by solutions containing the indicated cations (120–125 mM). Symbols are as in Fig. 1. Data points are means ± SEM of (*n*) experiments. (*A*) I–V plots measured in the presence of different organic cations. (*B*) Comparison of I–V plots measured with Na^+, Li^+, $Form^+$, $Acet^+$, and Cs^+.

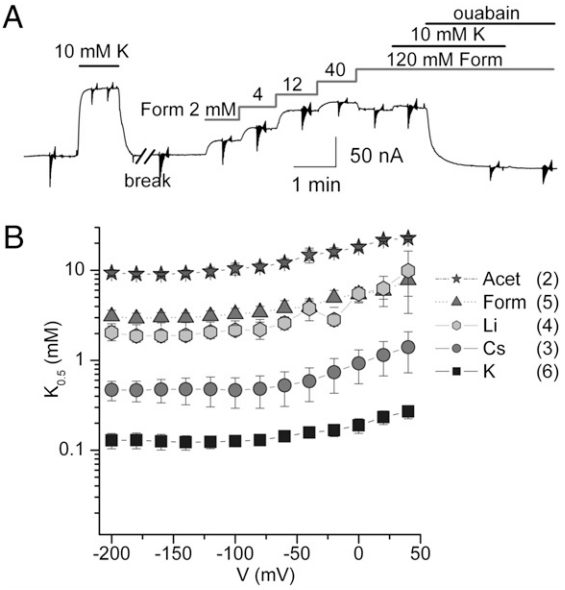

Fig. 4. Cation activation of outward currents. (*A*) Continuous recording at V_h = −50 mV from a Na-loaded oocyte. Initial application of 10 mM K^+_o (in NMG^+_o) gave an estimate of the maximal outward pump current. After K^+ washout (i.e., during the break in the time scale), the oocyte was superfused with other test external-cation solutions. Shown after the break are step increments in [$Form^+_o$] (adjusting [NMG^+_o] to achieve 120 mM) from 0–120 mM [$Form^+_o$]. At 120 mM, $Form^+_o$ induced an ouabain-insensitive inward current of unknown nature. Addition of 10 mM K^+_o to the 120-mM $Form^+_o$ solution increased outward current only slightly. Ouabain inhibited outward current in both the presence and absence of K^+_o. (*B*) Voltage dependence of the half-maximal constant ($K_{0.5}$) for activation of outward current in the absence of external Na^+_o. For each ion, the Hill plots for $K_{0.5}$ estimation considered only concentrations that did not activate significant pump-independent currents ([K^+_o] ≤10 mM, [Cs^+_o] ≤20 mM, and [cation^+_o] ≤40 mM for the other three). Data points are means ± SEM of (*n*) experiments in different oocytes.

These observations require structural rationalization of the occluded state with bound $Acet^+$. In particular, one may ask if $Acet^+$ can reasonably bind to a K^+-selective site and, if so, what circumstances govern this process at the atomic level. We used computational modeling to address these questions. A series of configurations were generated with two $Acet^+$ molecules docked into the K^+ sites of the X-ray structure (Protein Data Bank 2ZXE) (14) in random orientations. A few complexes were followed by molecular dynamics (MD) simulation. Several orientations produced stable configurations with modest protein distortion within a short (200 ps) simulation time, indicating that this procedure does not allow determination of the relative probability of the different arrangements.

One plausible orientation was chosen arbitrarily to perform a more extensive (20 ns) MD simulation to assess the magnitude

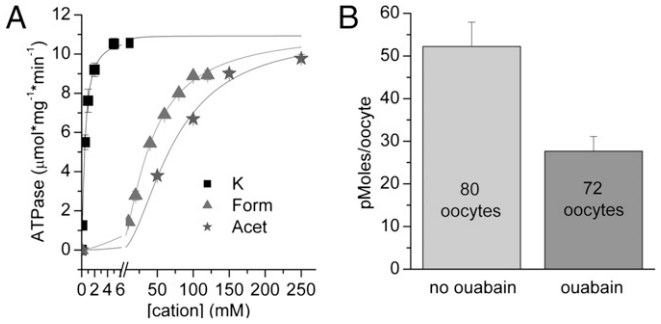

Fig. 5. Organic cations act as K^+ congeners. (*A*) ATPase activity from purified sheep kidney. Na/K pump preparations at different [Form$^+$], [Acet$^+$], or [K^+] in the presence of 30 mM Na^+ and 3.3 mM ATP (*Methods*). Data points are means ± SEM from three experiments with triplicate measures. Continuous lines represent the Hill equation fitted to the average data with best-fit parameters. For K^+, $V_{max} = 10.9 \pm 0.2$ μmol·mg^{-1}·min^{-1}, $K_{0.5} = 0.50 \pm 0.03$ mM, $n = 1.2 \pm 0.1$; for Form$^+$, $V_{max} = 11.2 \pm 0.2$ μmol·mg^{-1}·min^{-1}, $K_{0.5} = 42 \pm 6$ mM, $n = 1.4 \pm 0.26$; and for Acet$^+$, $V_{max} = 10.9 \pm 0.2$ μmol·mg^{-1}·min^{-1}, $K_{0.5} = 73 \pm 6$ mM, $n = 1.8 \pm 0.1$. (*B*) C^{14}-labeled Acet$^+$ uptake measured in *Xenopus* oocytes expressing wild-type α1 + β3 Na/K pumps. Uptake (*Methods*) was measured in the presence of 10 mM $Acet^+_o$ and 110 mM NMG^+_o, in the absence (light gray) or presence (dark gray) of 10 mM ouabain.

of structural distortion induced by the organic cation within the binding site. Fig. 6*A* shows the final snapshot after the simulation, compared in Fig. 6*B* with the corresponding structure with two bound K^+ ions after a comparable 20-ns MD simulation.

The rmsd of nonhydrogen atoms of the key residues participating in the coordination averaged from the MD trajectory is on the order of 1.5 Å (Fig. S7*A*), showing that the binding sites are minimally disturbed by the bound organic cations. One noticeable difference between the K^+-bound X-ray structure and the Acet$^+$-bound configuration generated by the simulation is the orientation of residue Asp^{815} (shark Na/K-ATPase numbering), whose rotation away from site I allows two water molecules to participate in coordinating Acet$^+$, as illustrated by the radial distribution function for the oxygen from water as a function of the distance to the carbon of the Acet$^+$ (Fig. S7*B*). Coordination

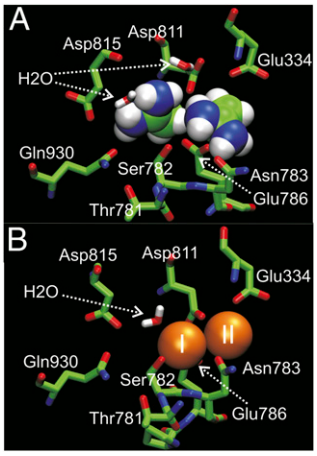

Fig. 6. Cytoplasmic view of the structural model of acetamidinium$^+$ occlusion. (*A*) Final configuration following a 20-ns MD simulation started from a model of the complex with docked Acet$^+$. (*B*) Ion-binding pocket following a 20-ns MD simulation on the crystallographic structure with K^+ ions bound [Protein Data Bank 2ZXE (14)]. Detailed methodological information is given in *SI Methods*.

of the K^+ ions by water molecule also is observed in the K-bound structure (Fig. 6*B*). (14)

Discussion

Selectivity of the Na-Exclusive Site III. The location and nature of the Na-exclusive site III has yet to be determined unequivocally. On the basis of homology modeling (8) and mutagenesis (6), earlier reports suggested that this site was formed by several oxygen-containing residues between transmembrane (TM) segments TM5, TM6, and TM9. However, a recent report (9) shows that both the VDI in the presence of Na^+_o and K^+_o and the inward H^+ leak in the absence of Na^+_o and K^+_o vanish when the mutation D930N (in TM8) is introduced of the human α2 subunit (D933 in the shark α1). Because both these phenomena are attributed to site III, these findings suggest that site III may be located elsewhere than previously thought. The authors proposed that ions access site III through a pathway different from the one used to access sites I and II. Although our results do not identify the location of site III or the pathway leading to it, they set constraints on the determinants of its selectivity.

In agreement with the discussion above, the identical voltage dependence of maximal K^+_o-activated Na/K pump current at 125 mM Na^+_o and that observed as ouabain-sensitive current at 20 mM K^+_o (Fig. S4) corroborates that the VDI produced by Na^+_o interaction at site III is noncompetitive with K^+_o. Therefore the 50% higher inhibition at −200 mV in 125 mM Na^+_o compared with 125 mM NMG^+_o suggests that this large cation cannot enter the first Na^+ release site. The small (~25%) reduction observed in NMG^+_o probably arises from a mild voltage dependence attributed to the E1–E2 transition (3).

What constraints are required for an ion to induce a positive slope in the I_P–V curve? If the access channel merely allowed any ion that fits into it to reach the Na-exclusive site before the second and third Na^+ ions are externally released from the shared sites, then all sufficiently small external cations should produce Na-like VDI. It is clear that 120 mM Gua^+_o produced an I_P–V curve with a positive slope at high K^+_o (Fig. 1*A* and Fig. S4). The ionic radius of Gua$^+$ is larger than either K^+ or Cs^+, but, unlike Cs^+ and K^+, Gua$^+$ is not excluded from the site (Fig. 1 *A* and *B*). This observation suggests that it may be the larger hydrated forms of the metal ions that enter the Na^+-exclusive site, similar to proposals of voltage-dependent Na-channel (VNaC) selectivity by Hille (18), where hydrated K^+ and its congeners cannot enter the Na-selective channel. However, overall size (including hydration) cannot fully explain VDI by cations, because more inhibition was observed with $Mgua^+_o$ than with the smaller cations MA^+_o and $Acet^+_o$ (Fig. 1*C*). Furthermore, because these three cations have a methyl group, ion selectivity of the access channel involved in VDI is not identical to selectivity in VNaC, where ions with a methyl group do not permeate (15). Compared with Acet$^+$, Gua$^+$ derivatives have an additional $-NH_2$ group connected to the central carbon atom. This addition increases the number of resonance structures available to delocalize the positive charge, possibly making them chemically closer than the other ions to a hydrated Na^+. Presumably, these chemical characteristics allow Gua$^+$ to mimic Na^+ with one or two associated water molecules as it moves along the access pathway. In agreement with these results, an earlier homology model illustrates an Na^+ ion associated with two water molecules in the putative site III (8).

Na/K pump uncoupled ion fluxes. In the absence of external Na^+ and K^+, two ouabain-sensitive, pH_o-dependent oppositely directed currents were observed: an uncoupled outward current observed in NMG^+_o solutions at pH 8.6 (Fig. 2 and Fig. S5), probably resulting from electrogenic uncoupled Na^+ efflux (a conclusive determination of its nature exceeds the scope of this report), and an uncoupled inward current observed during negative voltage pulses, which has been associated with an ion pathway through site III.

The inward current observed at pH_o 7.6 and below in 125 mM NMG^+_o (an ion that does not interact with the binding sites) (19, 20) is thought to represent electrochemically dissipative H^+ flow through site III of the Na,K-ATPase (9, 12, 13). This transport mode appears too slow and rate limited by protein conformational changes to represent simple ion flow through an ion channel (12, 21).

The threefold larger inward current observed in the absence of Na^+_o and K^+_o with 120 mM Gua^+_o as compared with 125 mM NMG (10) indicates that, like H^+, Gua^+_o enters and passively permeates the pump or that Gua^+_o increases the H^+ flow allosterically. The pH_o and cation dependence of inward currents indicates that Gua^+_o (Figs. 2*B* and 3*A* and Fig. S5), $Agua^+_o$, and $Mgua^+_o$ (Fig. 3*A* and Fig. S6) are all passively transported. Although the impossibility of completely eliminating protons from the solution makes irrefutable conclusions difficult, thermodynamics makes it unlikely that Gua^+_o acts only to catalyze H^+ transport. At pH_o 8.6, where no inward current was observed in NMG^+_o, the V_{rev} of the current depended strongly on [Gua^+_o] (Fig. 2*B*). If protons were the only permeant cation in 125 mM Gua^+_o at pH_o 8.6, a negative V_{rev} (~−58 mV) would be predicted, but a V_{rev} of ~0 mV was observed (accumulation of Gua^+ on the intracellular side may explain the absence of a positive V_{rev} in Gua^+_o). Moreover, we observed no significant change in V_{rev} with a 100-fold change in [H^+_o] at constant 125 mM Gua^+_o (Fig. 2*A*), indicating that H^+ and Gua^+ may traverse the same pathway. This observation suggests that the permeating chemical species in NMG^+_o solutions may, in fact, be H_3O^+, more similar in size to hydrated Na^+ or Li^+ (Fig. S2), which are bona fide substrates for binding and occlusion at the Na-exclusive site.

If downhill H^+ and Gua^+ transport is through site III (13), a paradoxical observation is that H^+ and Gua^+ can leak through normal Na/K pumps, although the more common substrate Na^+ cannot (nor can Li^+). Although, as yet, there is no definitive answer for this puzzle, we propose, based on our results and the current understanding of pump function, that sites I and II act as a "switch" that controls both access and binding to site III. Consistent with this interpretation is the observation that inward current is absent in the presence of external cations that can be occluded at the shared sites, namely K^+, Cs^+, Li^+, Na^+, $Form^+$, or $Acet^+$. The possibility that, in the presence of Na^+_o, binding to site III is responsible for inhibition of the inward current seems unlikely, because the $K_{0.5}$ for site III, responsible for most VDI at saturating K^+_o, is ~125 mM at −160 mV (Fig. S4), but 125 mM Na^+_o completely abolished inward currents (Fig. 3).

Thus, under conditions of reduced ion occlusion at the shared sites, the pathway that leads to site III appears to be open, but tight binding does not occur because Na-like binding to the shared sites (with relative high affinity, compared with the affinity of the Na-exclusive site) is a prerequisite. In contrast, K^+-like binding to sites I and II shuts access to site III, as evidenced in the K^+-bound structure (14). In good agreement with this hypothesis, Gua^+ derivatives that interact with the shared sites but are not occluded actually enhance the inward uncoupled current. This observation may indicate that lack of ion occlusion at the shared sites is the event that stimulates an inward leak at very negative voltages. Protonation of residues at this site may induce a similar, Gua^+-like effect when pH_o is lowered, making the pump "leaky" to protons and Na^+, as reported previously (22). Considering the sequential nature of external ion-binding reactions at the shared sites for both Na^+ (3, 4) and K^+ (23) ions, it is tempting to propose that binding of nonoccluded Gua^+ or protonation of residues in the first ion-binding site dramatically reduces affinity for the second ion-binding site, making the pump leaky. However, determining which binding site(s) the ions interact with during permeation, the exact mechanism inducing this uncoupled inward current, and the actual structural nature of the pathway will require future investigation.

Ion selectivity of outward-facing shared sites. It is well established that K^+, Rb^+, Cs^+, Li^+, and NH^+_4 all increase the rate of forward E2P hydrolysis compared with Na^+, which induces the slowest dephosphorylation rate (1). Perhaps the most surprising finding of the present study is that $Form^+_o$ and $Acet^+_o$ can act as K^+_o surrogates in the Na/K pump cycle (Figs. 3*B*, 4, and 5).

The large outward currents observed with $Acet^+_o$ (80% of K^+_o-induced currents; Fig. 3*B*) suggests that two $Acet^+_o$ ions may be exchanged for three Na^+_i ions, thus preserving the normal 3:2 stoichiometry of the pump. However, the total ouabain-sensitive uptake (~25 pmole per oocyte) (Fig. 5*B*) was ~20-fold lower than would be expected if all injected oocytes expressed exogenous pumps. At 10 mM $Acet^+$ we would expect a current of ~50 nA (given that the $K_{0.5Acet}$ is ~20 mM at 0 mV and the maximum $Acet^+$-induced current is ~20% lower than in K^+_o, which typically is ~200 nA). A strict 3:2 stoichiometry should produce an uptake of 500 pmole, and the observed ~20-fold discrepancy may reflect different factors, such as lack of exogenous expression in some oocytes, depletion of intracellular Na^+ during the long uptake reaction assays (5 min) compared with the relatively short electrical measurements (30–60 s), and loss of $Acet^+$ through leak pathways during washout of the radioactive uptake solution. Further evaluation of uptake under two-electrode voltage clamp in individual oocytes will be required to confirm stoichiometry.

The K^+-like transport of $Form^+$ and $Acet^+$ provides evidence of their interaction and occlusion at the shared sites. Gua^+ also may interact with at least one of the two shared sites but without allowing full occlusion, as indicated by the reduction in apparent affinity for K^+ (Fig. S3). The small structural protein distortions and the stability of the two $Acet^+$ cations in the binding pocket observed during a 20-ns MD simulation (Fig. 6*A*) suggests that occlusion is possible without major alteration of residues at the ion-binding sites. Although more extensive computational sampling would be required to ascertain fully the stability of the two $Acet^+$ cations in the binding pocket, the lack of significant distortions in the protein upon binding of the organic cation $Acet^+$ suggests that the shared sites must be able to achieve their high specificity via a surrounding molecular architecture that is able to remain fairly flexible. This observation challenges the concept of rigid structural models reminiscent of "host–guest" chemistry (24) in which the selectivity of the binding sites must necessarily be attributed to the precise and unique arrangement of coordinating ligands.

Such a structural explanation of selectivity, traditionally called the "snug-fit" mechanism in the field of permeation and ion channels (25), relies on the ability of the structure to retain its local conformation very precisely, a condition that cannot be fulfilled when the protein also must be able to stay sufficiently flexible to perform its function (26). Therefore, in retrospect, it may not be surprising that the underlying mechanism of ion selectivity in the Na/K pump is more complex than the mechanisms observed in ion channels and transporters that are not required to change selectivity as they function (27). Considering the high similarity between the mechanisms of function and the ion-binding site residues of the Na/K pump, the gastric and nongastric H/K pumps, and SERCA, it is likely that the results presented here may contribute to the understanding of ion selectivity in other ion pumps.

Methods

Oocyte Preparation and Molecular Biology. Oocytes were isolated enzymatically as described (10), injected with an equimolar mixture of *Xenopus* α1 (25 ng) and *Xenopus* β3 cRNAs, and kept at 16 °C for 2–6 d until use in a solution containing 100 mM NaCl, 2 mM KCl, 1.8 mM $CaCl_2$, 1 mM $MgCl_2$, and 5 mM Hepes, supplemented with horse serum (Sigma) and an antimycotic/antibiotic mixture (Anti-Anti; Gibco). For electrophysiological experiments, the double-mutant α1-Q120R-N131D was used because of its lower ouabain sensitivity (IC_{50} ~100 μM) that allows reversible inhibition of exogenous pumps during the experiment and distinction from ouabain-sensitive endogenous pumps that remained continuously inhibited after

preincubation with ouabain. For ^{14}C-Acet$^+$ uptake experiments, oocytes were injected with wild-type α1 to facilitate irreversible inhibition with ouabain while boosting the signal, because the uptake through endogenous pumps is measured also.

Solutions. Oocytes were Na^+-loaded by a 1- to 2-h incubation in a solution containing 90 mM Na-sulfamate, 20 mM Na-Hepes, 20 mM tetraethylammonium chloride, and 0.2 mM EGTA (pH 7.6) and then were transferred to a K^+-free OR2 solution containing 10–20 μM ouabain and 82.5 mM NaCl, 1.8 mM $CaCl_2$, 1 mM $MgCl_2$, and 5 mM Hepes until recording. Metal cation external solutions were composed of 125 mM cation-OH, 10 mM Hepes, 5 mM $Ba(OH)_2$, 1 mM $Mg(OH)_2$, 0.5 mM $Ca(OH)_2$ (pH 7.6 with methanesulfonic acid). External solutions containing organic cations were composed of (in mM)120 main cation-Cl salt, 10 mM Hepes, 5 mM $BaCl_2$, 1 mM $MgCl_2$, 0.5 mM $CaCl_2$ (pH 7.6 with ~5 mM extra NMG). Where pH_o was modified, all solutions (pH 6.6, 7.6, and 8.6, respectively) contained 10 mM each of Hepes, MES, and TAPS to attain buffering in all ranges. Final pH in these solutions was achieved by adding HCl or NMG^+. To measure K_o^+-activated current, up to 20 mM K^+ was added to the external solutions from a 3-M K-methanesulfonic acid stock.

Two-Electrode Voltage Clamp. The two-electrode voltage clamp was made using an OC-725C amplifier (Warner Instruments), a Digidata 1440 A/D board, a Minidigi 1A, and pClamp 10 software (Molecular Devices). Signals were filtered at 2 kHz and digitized at 10 kHz. Resistance of current and voltage microelectrodes were 0.5–1 MΩ and 1–2 MΩ, respectively (filled with 3 M KCl).

Radiolabeled ^{14}C-Acetamidine Uptake. Uptake was performed on Na-loaded oocytes 2–3 d after injection of cRNA encoding wild-type α1β3 pumps. ^{14}C-acetamidine HCl (40–60 mCi/mmol) (Moravek Biochemicals) was added from a 12-mM stock in water to a solution of 10 mM cold Acet$^+$ and 115 mM NMG (pH 7.6). Oocytes of healthy appearance were selected after Na^+ loading, and groups of 20 oocytes were incubated in the absence or presence of 1 mM ouabain. After 5 min, oocytes were washed in OR2 solution with ouabain, treated with SDS, and vortexed. Radioactivity was determined via liquid scintillation spectroscopy in groups of three to six oocytes. Minimal residual radioactivity was measured in empty tubes and subtracted. The specific uptake equals total corrected counts divided by the number of oocytes per tube.

Enzyme Activity. Na,K-ATPase was purified from sheep kidney, and ouabain-sensitive ATP hydrolysis was determined as described previously with minor modifications (28). Briefly, assays were performed in a standard medium containing 1 mM EGTA, 24 mM NaCl, 3 mM $MgCl_2$, 3.3 mM Na_2ATP, 50 mM imidazole (pH 7.4, 25 °C), and 0.5 μg/mL purified enzyme. Concentrations of K^+, Acet$^+$, and Form$^+$ were as indicated (Fig. 5). The suspension was incubated at 37 °C for 15 min, and the liberation of PO_4 was measured as described in ref. 28. Specific activity was the difference between ATP hydrolysis measured in the absence and presence of 0.5 mM ouabain. Total salt concentration was kept constant with NMG^+.

Atomic Model and Simulations. MD simulations of a reduced atomic system representing the region of the ion-binding sites of the Na/K pump were carried out using the generalized solvent boundary potential (GSBP), which incorporates the long-range electrostatic influence of the surroundings via static and reaction fields (29). Atoms within a 15-Å radius centered on the ion-binding sites were defined as the inner GSBP region, yielding a reduced system of ~4,000 atoms. The inner region is extended by 3 Å to define a smooth, spherical dielectric cavity. The protein atoms located in the 3-Å shell and those within the extended inner spherical region (≤18 Å) linked via 1–3 bonds with the outer region (>18 Å) were fixed according to a group-based criterion. All other atoms, including the protein ions, and solvent molecules in the inner region, were allowed to move during the MD trajectory as explained in *SI Methods*.

ACKNOWLEDGMENTS. This work was supported by start-up funds from Texas Tech University Health Science Center and by American Heart Association Grant BGIA2140172 (to P.A.) and by National Institutes of Health Grants DK083859 (to C.G.) and GM062342 (to B.R.).

1. Post RL, Hegyvary C, Kume S (1972) Activation by adenosine triphosphate in the phosphorylation kinetics of sodium and potassium ion transport adenosine triphosphatase. *J Biol Chem* 247:6530–6540.
2. Sachs JR (1986) The order of addition of sodium and release of potassium at the inside of the sodium pump of the human red cell. *J Physiol* 381:149–168.
3. Heyse S, Wuddel I, Apell HJ, Stürmer W (1994) Partial reactions of the Na,K-ATPase: Determination of rate constants. *J Gen Physiol* 104:197–240.
4. Holmgren M, et al. (2000) Three distinct and sequential steps in the release of sodium ions by the Na+/K+-ATPase. *Nature* 403:898–901.
5. Gadsby DC, Nakao M (1989) Steady-state current-voltage relationship of the Na/K pump in guinea pig ventricular myocytes. *J Gen Physiol* 94:511–537.
6. Li C, Capendeguy O, Geering K, Horisberger JD (2005) A third Na+-binding site in the sodium pump. *Proc Natl Acad Sci USA* 102:12706–12711.
7. Peluffo RD (2004) Effect of ADP on Na(+)-Na(+) exchange reaction kinetics of Na,K-ATPase. *Biophys J* 87:883–898.
8. Ogawa H, Toyoshima C (2002) Homology modeling of the cation binding sites of Na+K+-ATPase. *Proc Natl Acad Sci USA* 99:15977–15982.
9. Poulsen H, et al. (2010) Neurological disease mutations compromise a C-terminal ion pathway in the Na(+)/K(+)-ATPase. *Nature* 467:99–102.
10. Yaragatupalli S, Olivera JF, Gatto C, Artigas P (2009) Altered Na+ transport after an intracellular alpha-subunit deletion reveals strict external sequential release of Na+ from the Na/K pump. *Proc Natl Acad Sci USA* 106:15507–15512.
11. Wang X, Horisberger JD (1995) A conformation of Na(+)-K+ pump is permeable to proton. *Am J Physiol* 268:C590–C595.
12. Meier S, Tavraz NN, Dürr KL, Friedrich T (2010) Hyperpolarization-activated inward leakage currents caused by deletion or mutation of carboxy-terminal tyrosines of the Na+/K+-ATPase alpha subunit. *J Gen Physiol* 135:115–134.
13. Li C, Geering K, Horisberger JD (2006) The third sodium binding site of Na,K-ATPase is functionally linked to acidic pH-activated inward current. *J Membr Biol* 213:1–9.
14. Shinoda T, Ogawa H, Cornelius F, Toyoshima C (2009) Crystal structure of the sodium-potassium pump at 2.4 A resolution. *Nature* 459:446–450.
15. Hille B (1971) The permeability of the sodium channel to organic cations in myelinated nerve. *J Gen Physiol* 58:599–619.
16. Cornelius F (1990) Variable stoichiometry in reconstituted shark Na,K-ATPase engaged in uncoupled efflux. *Biochim Biophys Acta* 1026:147–152.
17. Hemsworth PD, Whalley DW, Rasmussen HH (1997) Electrogenic Li+/Li+ exchange mediated by the Na+-K+ pump in rabbit cardiac myocytes. *Am J Physiol* 272: C1186–C1192.
18. Hille B (1971) The hydration of sodium ions crossing the nerve membrane. *Proc Natl Acad Sci USA* 68:280–282.
19. Gatto C, Helms JB, Prasse MC, Arnett KL, Milanick MA (2005) Kinetic characterization of tetrapropylammonium inhibition reveals how ATP and Pi alter access to the Na+-K+-ATPase transport site. *Am J Physiol Cell Physiol* 289:C302–C311.
20. Gatto C, et al. (2006) Similarities and differences between organic cation inhibition of the Na,K-ATPase and PMCA. *Biochemistry* 45:13331–13345.
21. Rettinger J (1996) Characteristics of Na+/K(+)-ATPase mediated proton current in Na(+)- and K(+)-free extracellular solutions. Indications for kinetic similarities between H+/K(+)-ATPase and Na+/K(+)-ATPase. *Biochim Biophys Acta* 1282:207–215.
22. Vasilyev A, Khater K, Rakowski RF (2004) Effect of extracellular pH on presteady-state and steady-state current mediated by the Na+/K+ pump. *J Membr Biol* 198:65–76.
23. Forbush B,, 3rd (1987) Rapid release of 42K or 86Rb from two distinct transport sites on the Na,K-pump in the presence of Pi or vanadate. *J Biol Chem* 262:11116–11127.
24. Dietrich B (1985) Coordination chemistry of alkali and alkaline-earth cations with macrocyclic ligands. *J Chem Educ* 62:954–964.
25. Bezanilla F, Armstrong CM (1972) Negative conductance caused by entry of sodium and cesium ions into the potassium channels of squid axons. *J Gen Physiol* 60:588–608.
26. Noskov SY, Roux B (2007) Importance of hydration and dynamics on the selectivity of the KcsA and NaK channels. *J Gen Physiol* 129:135–143.
27. Noskov SY, Roux B (2008) Control of ion selectivity in LeuT: Two Na+ binding sites with two different mechanisms. *J Mol Biol* 377:804–818.
28. Gatto C, Thornewell SJ, Holden JP, Kaplan JH (1999) Cys(577) is a conformationally mobile residue in the ATP-binding domain of the Na,K-ATPase alpha-subunit. *J Biol Chem* 274:24995–25003.
29. Im W, Berneche S, Roux B (2001) Generalized solvent boundary potential for computer simulations. *J Chem Phys* 114:2924–2937.